

# Interfaze: The Future of AI is built on Task-Specific Small Models

Harsha Vardhan Khurdula  
JigsawStack, Inc.  
San Francisco, CA, USA  
harsha@jigsawstack.com

Vineet Agarwal  
JigsawStack, Inc.  
Durgapur, WB, India  
vineet@jigsawstack.com

Yoeven D Khemlani  
JigsawStack, Inc.  
San Francisco, CA, USA  
yoeven@jigsawstack.com

**Abstract**— We present **Interfaze**, a system that treats modern LLM applications as a problem of building and acting over *context*, not just picking the right monolithic model. Instead of a single transformer, we combine (i) a stack of heterogeneous DNNs paired with small language models as perception modules for OCR involving complex PDFs, charts & diagrams, and multilingual ASR with (ii) a context-construction layer that crawls, indexes, and parses external sources (web pages, code, PDFs) into compact structured state, and (iii) an action layer that can browse, retrieve, execute code in a sandbox, and drive a headless browser for dynamic web pages. A thin controller sits on top of this stack and exposes a single, OpenAI-style endpoint: it decides which small models and actions to run and always forwards the distilled context to a user-selected LLM that produces the final response.

On this architecture, **Interfaze-Beta** achieves 83.6% on MMLU-Pro, 91.4% on MMLU, 81.3% on GPQA-Diamond, 57.8% on LiveCodeBench v5, and 90.0% on AIME-2025, along with strong multimodal scores on MMMU (val) (77.3%), AI2D (91.5%), ChartQA (90.9%), and Common Voice v16 (90.8%). We show that most queries are handled primarily by the small-model and tool stack, with the large LLM operating only on distilled context, yielding competitive accuracy while shifting the bulk of computation away from the most expensive and monolithic models.

## I. INTRODUCTION

General-purpose LLMs have impressive breadth, but deployed systems need more than next-token prediction. They must *see* the world (OCR, object detection, speech recognition, classification), *build and maintain* external context (indexes, caches, code, tools), and then *reason* over that context. Running a single frontier model over raw inputs: a full PDF, a long audio file, or an entire website which is often neither economical nor robust [2], [3]. Benchmarks that stress reasoning and multimodal understanding rather than memorization (MMLU-Pro, GPQA-Diamond, AIME-2025, MMMU, AI2D, ChartQA, Common Voice) make this gap explicit [10], [12]–[16], [26].

In practice, production systems already consist of heterogeneous deep networks and tools. Vision backbones handle object detection and segmentation; document models drive OCR and layout analysis; ASR and diarization stacks transcribe and segment audio; retrieval systems and lightweight classifiers gate search, safety, and domain routing [24], [26]. Large language models usually sit at the end of this chain: they are asked to reason over structured outputs rather than pixels or waveforms.

Recent work formalizes parts of this picture. Hybrid routing and cascades study when a small model is “good enough” and when to escalate to a larger one, using learned difficulty estimates and cost-aware policies [1]–[4]. Tool-augmented LLMs show gains when the model can call APIs, search, and run code [5]–[8], [22]. In parallel, small language models are used as plug-in specialists for retrieval, reranking, and domain-specific reasoning, and as compact models for edge settings [17]–[20], [23]. Yet most of these systems are described from the perspective of the large model or router. The concrete design of the small-model stack, i.e., which DNNs handle perception and classification, how their outputs are filtered and merged, and how they interface with scrapers and indexes is typically abstracted behind generic “tool calls,” making it difficult to reproduce or to see which pieces actually drive gains on multimodal and long-context tasks.

We adopt a systems perspective. We treat modern LLM applications as systems for building and acting over *context*, and we make the small DNNs and SLMs that build this context first-class citizens. **Interfaze** is a context-centric architecture with three parts:

- 1) a heterogeneous DNN and SLM stack for perception and classification across modalities (object detection, OCR, speech-to-text, text and image classification),
- 2) a context-construction layer that crawls, indexes, and parses external sources (web pages, code, PDFs, diagrams) into compact structured state, and
- 3) an action layer with a thin controller that selects which tools to run, compiles the resulting state into a bounded prompt, and hands that distilled context to a configured LLM that generates the final answer.

Our concrete instantiation, **Interfaze-Beta**, uses specialized models for the major perception and classification tasks (document understanding for OCR and layout, chart and diagram parsing, a multilingual ASR and diarization stack, and small transformers for text and image classification). These models cooperate with web search, indexing, scraping, and a sandbox to construct the context the final generalist LLM sees. We describe the architectures and roles of these components in detail and evaluate the resulting system across knowledge, reasoning, code, multimodal, and speech benchmarks.

We contribute the following:

- a context-centric system architecture that treats small

DNNs and SLMs for perception and retrieval as first-class components rather than opaque tools,

- a concrete instantiation, Interfaze-Beta, that integrates OCR, chart/diagram parsing, ASR/diarization, retrieval, and a sandbox behind a single endpoint,
- an empirical study showing that this stack achieves competitive or state-of-the-art results on challenging reasoning and multimodal benchmarks while keeping most compute on small models, and
- an analysis of the limitations of the current controller and context-construction strategy, highlighting delay and over-building of context as primary targets for future work.

## II. LITERATURE SURVEY

### A. Context is key

TABLE I

AVERAGE LONG-CONTEXT BENCHMARK PERFORMANCE FOR SEVERAL LLMs (ADAPTED FROM HRON [46]).

Model	1M ctx. score	128K ctx. score
gpt-4o-2024-11-20	50	60
gpt-4.1-alpha	55	75
o3-mini-2025-01-31	50	55
o1-2024-12-17	56	62
claude-3-7-sonnet	50	58
claude-3-7-sonnet-thinking	54	63
gemini-1.5-pro-002	56	67

Recent work suggests that *how* context is selected and organized matters more than simply enlarging a model or its window. A Databricks study on financial and corporate QA varies both retrieved document count and prompt length for long-context models such as GPT-4 Turbo and Claude 2, and observes gains only while the retrieved text remains dense and relevant; once loosely related passages dominate, quality degrades even when the full context fits [45]. In legal QA, Hron reports a similar pattern: feeding entire filings sometimes beats naive RAG over small snippets, but performance still drops on very long documents with dispersed evidence [46]. Xu et al. show that moderate context windows combined with retrieval can match or outperform larger long-context baselines as shown in Table I across knowledge and reasoning benchmarks [47]. Together, these results argue that context must be filtered, structured, and budgeted. We extend this view by building compact, schema-based state from perception models and retrieval before any LLM is invoked.

### B. Where routing falls short

Hybrid routing work asks *which* LLM to call, and when a smaller model is “good enough.” FrugalGPT proposes cost-aware cascades over proprietary models [2]; Hybrid LLM adds a router that predicts query difficulty and routes between a local small model and a larger cloud model [3]; Universal Model Routing generalizes this idea to changing expert pools [4]; and routed architectures show that many experts can remain idle unless explicitly activated [1]. In almost all cases the experts are text-only LLMs of different sizes and prices.

Vision, speech, OCR, and retrieval are treated as fixed utilities, if they are modeled at all. This leaves open how to route over a heterogeneous DNN stack, or how much quality and cost are driven by perception and context construction rather than by the final LLM. We steer away from routing to this broader stack: the controller chooses tool chains over OCR, ASR, diagram parsing, retrieval, and sandboxed code, while the final LLM is a fixed answerer over the constructed context.

### C. Tools and model composition

A second line of work studies LLMs that call external tools. Toolformer demonstrates that a large model can label its own training data with API calls and learn when to invoke calculators, search, or translation systems [5]. HuggingGPT treats a large model as a planner over a registry of specialist models hosted on Hugging Face [6]. Prompting patterns such as ReAct interleave reasoning steps with explicit tool calls [7], and frameworks like Chameleon treat models and tools as composable modules arranged in small pipelines or trees [8]. Surveys summarize emerging design patterns and failure modes in such systems [22]. In most of this work, tools are defined only by high-level function signatures; the underlying DNNs for OCR, chart and diagram parsing, ASR, and retrieval are abstracted away. This makes it difficult to see which parts of the perception stack matter for benchmarks such as AI2D, ChartQA, MMMU, or Common Voice, where reliably reading diagrams, charts, and speech is the core challenge [14]–[16], [26]. Interfaze keeps the tool interface but treats these perception and retrieval models as first-class components, specifying how they are wired into crawlers and indexes and how their outputs are merged into a shared schema.

### D. Small language models and specialization

A complementary thread argues that small language models (SLMs) can be effective specialists. Schick and Schütze show that small models can act as strong few-shot learners on narrow tasks with the right prompting and calibration [19], [41]. Subsequent work uses compact models as plugin components for retrieval and ranking, improving larger systems on targeted subtasks even when the small models are not competitive as general chat models [20]. Flipping Knowledge Distillation uses small domain experts to transfer their strengths into larger generalists [21], and recent position papers argue that for many agentic or tool-heavy workflows, small models are attractive due to lower latency and energy use [23]. Classic compression work such as DistilBERT and MobileBERT makes the same argument for mobile and edge deployment [17], [18]. Less explored is how to organize systems in which SLMs handle most of the perception and context-building work across modalities, rather than just classification or reranking. Interfaze targets this gap: in Interfaze-Beta, compact DNNs and SLMs handle OCR and document layout, chart and diagram parsing, speech recognition and diarization, and lightweight classification, while the large LLM sees only the distilled context produced by these specialists.

### III. INTERFAZE-BETA ARCHITECTURE

Interfaze-Beta has four components: an ingress stage, a small-model and perception stack, a context construction layer, and an action layer with a lightweight controller.

#### A. System overview

A user query enters as a request  $x$  that may contain text, images, audio, or references such as URLs or documents. The ingress stage normalizes the input, detects modalities, and runs fast safety and intent checks. The small-model stack then processes raw content (OCR and layout for documents, detection and parsing for images, ASR for audio, and classifiers for domain, topic, and risk). The context layer merges these outputs with web, code, and documentation indexes into a structured state  $c(x)$ . Finally, the action layer selects a sequence of tool calls and passes the distilled state to a configured LLM that returns the answer.

Large LLMs never see raw pixels, waveforms, or entire websites. They only see  $c(x)$  and a compact representation of the original query, so most compute is spent in small models and retrieval rather than in the largest models.

#### B. Small-model and perception stack

The perception stack is a collection of small, task-specific models for different modalities: document/OCR models extract text lines, layout, and bounding boxes; object and chart/diagram models recover regions of interest, axes, legends, and numeric series; a multilingual ASR system transcribes audio segments with timestamps; and lightweight text and image classifiers predict domain, task type, and safety labels.

These models are much smaller than the final LLMs, run on separate GPU pools with batching and caching, and are cheap enough to invoke before any LLM call. Each is trained on a mixture of public and proprietary data; in this paper we focus on how they feed context construction.

#### C. Context construction and backfilling

The context layer turns the ingress summary, perception outputs, and retrieval results into a compact structured state  $c(x)$  tailored to the request.

Depending on the query, we hit one or more indexes: code-heavy questions query a code index over open source and internal repositories; “how do I use this tool” questions query documentation; general web questions query a broader web index. For document or URL inputs, a crawler and parser fetch and normalize the page or PDF, then pass it through the perception stack for OCR, layout analysis, and extraction of figures and tables.

Because these sources are noisy and redundant, a context compiler (i) merges overlapping spans and entities from multiple tools, (ii) filters low-confidence detections or text, and (iii) scores candidate spans and relations for relevance to the query. The resulting shared schema has four fields:

- **observations**: short textual statements from documents, code, or search results,

- **entities**: typed spans, bounding boxes, and nodes (e.g., variables, labeled regions, or table cells),
- **relations**: links between entities, such as chart axes, legend entries, or text–figure references,
- **provenance**: URLs, document identifiers, hashes, and timestamps.

Each field has a fixed token budget, and the compiler uses simple learned scoring models plus heuristics to stay within that budget. In practice, this schema is where most of the gains for AI2D, ChartQA, MMMU, and Common Voice originate.

#### D. Offloading large-context work

Long inputs motivate the architecture. Passing a full multi-page PDF, an entire site, or hours of audio directly to a large LLM is expensive and brittle, so Interfaze-Beta offloads as much as possible to the small-model and retrieval stack.

For documents, a parser segments the file into pages and blocks; OCR and layout models convert each page into structured tokens and lines; a small retriever indexes these segments; and questions retrieve only a handful of relevant segments, which the compiler distills into observations and entities. For websites, a headless browser renders the page, a scraper removes boilerplate, and a DOM-aware extractor identifies sections, code blocks, and figures; queries hit this index instead of running a full-page LLM pass. For audio, a voice activity detector segments the stream into utterances, the ASR model transcribes each segment, and downstream components operate on transcripts and timestamps rather than on waveforms.

In all cases, the large LLM sees only a small subset of the total content. The distilled state  $c(x)$  is passed to the action layer, which exposes a small set of primitives (query an index, fetch and parse a URL or document, run a perception model, execute code in a sandbox, or call a generalist LLM). The controller orders these primitives using simple cost and latency estimates; in Interfaze-Beta the final LLM is fixed by deployment configuration rather than chosen per request.

#### E. Action layer and specialized model chain

The action layer and specialized model chain make the system look like a single model to downstream developers.

A small controller sits on top of these primitives. Given the ingress summary and current input, it predicts a coarse task type and decides which indexes to query, whether to invoke additional perception passes, and whether to run code in the sandbox. Each decision corresponds to choosing a tool chain, i.e., which actions to invoke (retrieval only, retrieval plus code, extra perception passes) and which small models are active along that chain.

Every chain ends by calling a generalist LLM over the distilled context, so there is no learned gating between small and large LLMs and no path that skips the final model. The controller is trained on offline tuples of requests, tool chains, and pass/fail labels, and at inference prefers chains that satisfy a minimum predicted quality threshold while approximately minimizing a proxy for small-model cost and tail latency. If a

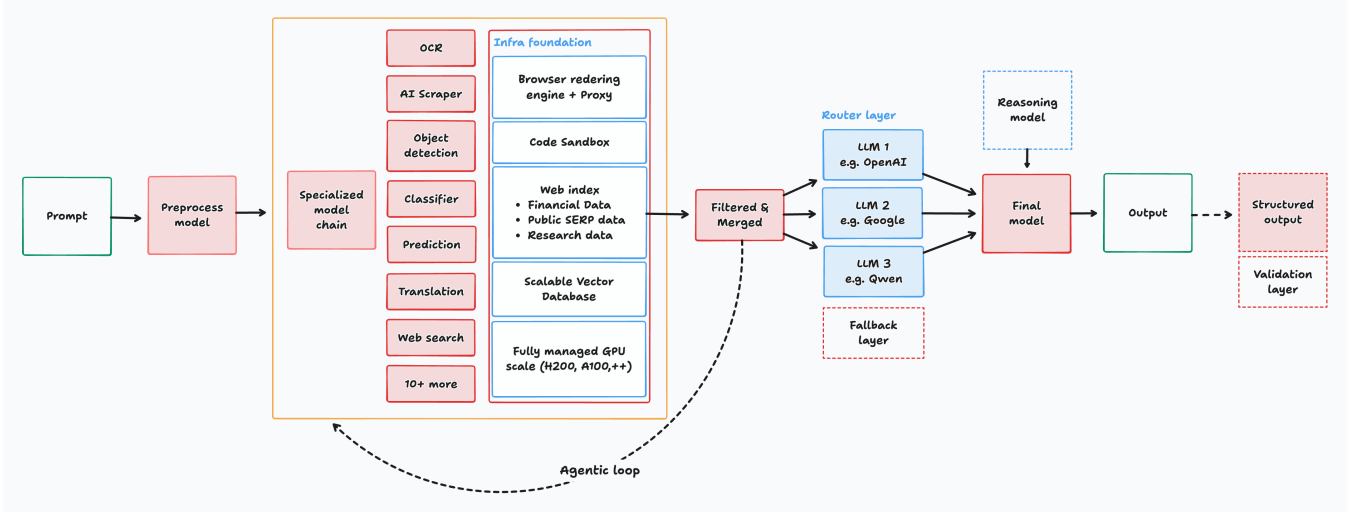


Fig. 1. Interfaze Architecture

chosen chain fails or times out, a fallback mechanism selects the next best feasible chain.

#### IV. PERCEPTUAL ENCODERS AT THE VISION-AUDIO INTERFACE

We treat raw audio, images, and documents as high-dimensional perceptual signals that must be encoded before any language model is invoked. Following large-scale work in speech recognition, speaker modeling, OCR, and visual grounding, we map waveforms to time-frequency representations that resemble low-resolution images, and we apply compact convolutional or time-delay encoders to them [27], [28]. Similar encoders operate on rasterized pages and screenshots. Lightweight heads predict tokens, languages, speaker embeddings, and geometric structure, while neural voice activity detectors segment continuous streams into manageable chunks [30], [31]. The resulting JSON state: utterance text with timestamps and speaker labels, text lines with bounding boxes, and object or GUI regions, feeds the context compiler and action layer in Section III.

In **Interfaze-Beta**, these perceptual modules are implemented as small, task-specific models trained in-house on a mixture of public and proprietary data. We describe them at the level of architecture and signal processing rather than dataset curation or model weights.

##### A. ASR with Diarization

Given an input waveform  $x(t)$  sampled at 16 kHz, the automatic speech recognition (ASR) branch applies a short-time Fourier transform

$$X(\tau, \omega) = \sum_n x[n] w[n - \tau] e^{-j\omega n},$$

where  $w$  is a window function and  $\tau$  indexes analysis frames. A mel filterbank  $M \in \mathbb{R}^{F \times K}$  aggregates squared magnitudes into  $F$  perceptual bands, and we compute log-mel features

$$z_{f,\tau} = \log((M|X(\tau, \cdot)|^2)_f + \epsilon),$$

which form a low-resolution time-frequency image [27], [30]. An encoder  $f_\theta$ , implemented as a stack of convolutional and self-attention blocks, maps the sequence  $z_{1:T}$  to hidden states  $h_{1:T} = f_\theta(z_{1:T})$ .

A sequence-to-sequence decoder  $g_\phi$  with cross-attention predicts subword tokens. At step  $t$ ,

$$p_\phi(y_t | y_{<t}, h_{1:T}) = \text{softmax}(W o_t + b),$$

where  $o_t$  is the decoder output and  $(W, b)$  are learned parameters. We train with teacher forcing and cross-entropy over transcriptions, optionally with a multilingual objective, and use greedy or low-beam decoding for low latency. For long recordings, a compact neural voice activity detector operates on short windows of  $z_{1:T}$ , producing framewise speech probabilities  $\hat{v}_\tau \in [0, 1]$  that are thresholded and merged into segments [30], [31]. Each segment is transcribed independently, bounding sequence length and enabling streaming.

Language conditioning is provided by a small time-delay network on frame-level features. It aggregates statistics over time and outputs a posterior  $p(\ell | z_{1:T})$  over languages. We convert the argmax language into a special token prepended to the decoder input. This improves multilingual recognition and stabilizes downstream task understanding while keeping the language detector small enough to run alongside VAD and ASR on the same GPU.

A diarization branch infers *who spoke when*. The raw audio is converted to mono at 16 kHz, bandpass-filtered, and amplitude-normalized. From this signal we compute cepstral or mel-spectral features  $u_{1:T}$ , and a segmentation network  $s_\psi$  produces framewise probabilities of speaker change or speech activity. Thresholding and merging active frames yields candidate segments.

For each segment  $k$  with time span  $[t_k^{\text{start}}, t_k^{\text{end}}]$ , a speaker-embedding network  $e_\omega$  maps the corresponding frames into a fixed-dimensional vector

$$\mathbf{v}_k = e_\omega(u_{t_k^{\text{start}}:t_k^{\text{end}}}),$$

following the emphasized channel-attention time-delay design standard in speaker verification and diarization [28]. L2-normalized embeddings are clustered (for example with agglomerative clustering in cosine space and a learned stopping criterion), assigning a discrete speaker label  $s_k$  to each segment, in line with recent open-source diarization pipelines [29].

A lightweight postprocessing step aligns ASR and diarization in time. For each transcribed chunk with timestamps  $[a_i^{\text{start}}, a_i^{\text{end}}]$  and text  $y^{(i)}$ , we find the diarization segment  $k$  with maximum temporal overlap and attach its label  $s_k$ . This yields an ordered list of utterances

$$\{(s_k, a_i^{\text{start}}, a_i^{\text{end}}, y^{(i)})\}_{i=1}^N,$$

which we serialize into JSON and pass to the context compiler. In the **Interfaze** schema, each utterance becomes an observation with an associated speaker entity, temporal relations, and provenance pointing back to the audio URL and model configuration.

Crucially, the large language models in **Interfaze Beta** never operate on raw audio or spectrograms. They see only this structured, speaker-annotated transcript with timestamps and language tags. Small summarization specialists condense long transcripts into compact observations, and the configured generalist LLM operates only on this distilled state.

## B. Optical Character Recognition and Complex Document Parsing

Our document pipeline targets heterogeneous, multilingual inputs such as receipts, scientific papers with equations and figures, forms, and multi-page PDFs. Rather than passing raw pixels to a large vision-language model, we run a sequence of lightweight vision and sequence models that extract word-level text with geometry, reconstruct reading order, and optionally perform schema-guided extraction, drawing on recent ultra-lightweight OCR and layout models [32], [33], [36].

a) *Rasterization and page fan-out.*: Given an input document  $x$ , we determine whether  $x$  is an image or a PDF. For PDFs, a renderer converts each page into a high-resolution RGB image  $I_p \in \mathbb{R}^{H \times W \times 3}$  with a fixed scale factor so that small fonts remain legible after downsampling by the detector. Pages are processed independently and in parallel, and very small images are upscaled to ensure a minimum effective x-height.

b) *Detection-recognition cascade.*: For each page image  $I_p$ , a text detector produces oriented quadrilateral regions

$$\{(Q_i, s_i)\}_{i=1}^N, \quad Q_i \in \mathbb{R}^{4 \times 2}, s_i \in [0, 1],$$

where  $Q_i$  are corner coordinates and  $s_i$  detection confidences. The detector uses a convolutional backbone with a feature pyramid and a segmentation-style head that predicts differentiable text regions; post-processing extracts connected components and fits polygons [32]. This supports arbitrarily oriented text with limited parameters.

Each detected region is cropped and passed to a recognizer that maps a variable-width strip to a character sequence. A 2D convolutional encoder produces a feature map  $F_i \in \mathbb{R}^{C \times T}$ , which is collapsed across height and fed to a lightweight sequence model (transformer or gated convolution) to predict  $y_i = (y_{i,1}, \dots, y_{i,T_i})$  over a multilingual alphabet, trained with a cross-entropy or CTC-style loss and language-aware augmentation [32]. This yields triples  $(Q_i, y_i, s_i)$  with text, geometry, and confidence for each line.

c) *Line grouping and reading order.*: Detector outputs alone do not define a logical reading order in multi-column layouts with headers, footers, and marginalia. We build a graph whose nodes are detected lines and whose edges connect geometrically adjacent lines. Nodes carry polygons  $Q_i$  and centroids  $c_i$ ; edges are scored using vertical overlap, horizontal distance, and font-height similarity, approximating pairwise features from learning-based reading-order systems [34]–[36]. A greedy path-finding algorithm traverses this graph to form chains corresponding to sections and paragraphs.

Within each chain, we aggregate text and define an axis-aligned bounding box  $B_i$  enclosing  $Q_i$ . Per-line confidence is a length-weighted average of word scores, giving sequences

$$\ell_j = (\text{text}_j, B_j, \bar{s}_j, \{w_{j,k}\}_k),$$

where each word  $w_{j,k}$  has its own bounding box and confidence, either from a native character-box head or by interpolation along the line when only line-level geometry is available.

d) *Fine-grained bounds correction and structured extraction.*: Complex layouts and low-contrast regions can cause gaps or merged words. We therefore keep an optional secondary recognizer at higher resolution or with a different inductive bias. Its outputs are aligned with the primary detector using intersection-over-union on polygons and token-level string similarity. Missing boxes are filled by merging character boxes into a tight quadrilateral or by partitioning a line box  $B_j$  according to character offsets. When geometric evidence is inconsistent, a small language model receives page text and neighboring coordinates and predicts local adjustments, constrained to preserve the original reading order.

When downstream tasks require structured fields (for example invoices or forms), we optionally invoke a vision-language model that operates on the page image and a short schema description. OCR-free and layout-aware transformers show that multimodal encoders can map a document image directly to JSON [33], [37]. We adopt this in a constrained way: the vision-language model receives the page image, a compact summary of OCR output, and a schema expressed as a JSON template, and is trained to emit a structured response that respects the schema. To control cost, this stage is triggered only when aggregate OCR confidence falls below a threshold or when the user explicitly requests structured extraction.

e) *Integration with Interfaze context.*: The final OCR representation for a document  $x$  is a structured state  $c_{\text{ocr}}(x)$  that plugs into the context compiler in Section III-C.

Lines and words populate entities with text spans and bounding boxes; reading-order edges and figure references form relations; and schema-guided fields become high-confidence observations with explicit provenance (page indices, section ids, and image hashes). Routed LLMs in **Interfaze** answer questions about complex, multilingual documents using this compact, geometry-aware context rather than raw pixels.

### C. Open-Vocabulary Object Detection and GUI Layout Parsing

For visual grounding and graphical user interface (GUI) reasoning, we combine (i) an open-vocabulary detector that localizes objects from natural-language prompts, (ii) a segmentation module based on Segment Anything Model 2 (SAM 2), and (iii) a GUI-specific layout parser for text regions, icons, and interactive widgets [44].

a) *Open-vocabulary detection as joint image-text scoring.*: Let  $x \in \mathbb{R}^{H \times W \times 3}$  be an RGB image and  $p \in \mathcal{P}$  a natural-language prompt (for example “red submit button” or “navigation menu”). We use a compact vision-language encoder inspired by image-text pre-training with sigmoid-based contrastive losses [38]. An image encoder

$$\phi_v : \mathbb{R}^{H \times W \times 3} \rightarrow \mathbb{R}^{D \times K} \quad (1)$$

produces a grid of  $K$  visual tokens, and a text encoder

$$\phi_t : \mathcal{P} \rightarrow \mathbb{R}^D \quad (2)$$

maps the prompt to a  $D$ -dimensional embedding. We compute a spatial relevance map

$$s_k = \sigma\left(\frac{\phi_v(x)_k^\top \phi_t(p)}{\tau}\right), \quad k = 1, \dots, K, \quad (3)$$

where  $\sigma$  is the sigmoid function and  $\tau$  a learned temperature. During pre-training,  $s_k$  is supervised to be high when token  $k$  overlaps ground-truth regions for the prompt and low otherwise, using a multi-label logistic formulation [38]. At inference, contiguous high-score regions in the spatial grid are grouped and mapped back to image coordinates, yielding boxes

$$B(p, x) = \{b_i = (x_{\min}^{(i)}, y_{\min}^{(i)}, x_{\max}^{(i)}, y_{\max}^{(i)})\}_{i=1}^{N_p}. \quad (4)$$

Because prompts are free-form text, the same encoder can localize arbitrary concepts, including unseen and multilingual categories.

b) *Prompt-conditioned instance segmentation with SAM 2.*: We refine each box  $b_i$  into a pixel-precise mask using Segment Anything Model 2 (SAM 2), a hierarchical Vision Transformer for promptable segmentation [39]. Given  $x$  and  $b_i$ , SAM 2 produces

$$m_i = S(x, b_i) \in \{0, 1\}^{H \times W}, \quad (5)$$

where  $S$  is the segmentation network. SAM 2 builds a multi-scale ViT representation and a lightweight mask decoder that conditions on prompt tokens and relevant encoder features to predict  $m_i$  in a single forward pass [39]. We batch all box prompts  $\{b_i\}$  per image to amortize GPU cost. Each

object is represented by  $(b_i, m_i)$  plus prompt  $p$  and detection confidence.

c) *GUI text and icon detection.*: For GUI screenshots, we activate a specialized layout parser with two detectors. A text detector based on character-region awareness identifies high-density text regions [40]. It regresses activation maps  $Y_{\text{char}}$  and  $Y_{\text{aff}}$  for character centers and pairwise affinity; thresholding and grouping connected components in  $Y_{\text{char}} \cup Y_{\text{aff}}$  yields word-level detections and a YOLO tuned model for icons and web elements [42], [43].

## V. RESULTS AND DISCUSSION

We report accuracy on knowledge and reasoning (**MMLU-Pro**, **MMLU**), graduate science (**GPQA-Diamond**), competition math (**AIME-2025**), coding (**LiveCodeBench v5**), multimodal perception (**MMMU validation split**, **AI2D**, **ChartQA**), and multilingual speech (**Common Voice v16**) as seen in Table II [10], [12]–[16], [25], [26]. All results for Interfaze-Beta use the same tool-orchestrated stack with the OCR/ASR, retrieval, chart/diagram, and sandbox tools enabled.

Interfaze-Beta leads on **AIME-2025** (90.0), **MMLU** (91.38), and **AI2D** (91.51). It is close to the strongest public reports on **MMLU-Pro** (83.6 vs. 86.2 for Gemini 2.5 Pro) and **GPQA-Diamond** (81.31 vs. 84.4), while delivering solid scores on **MMMU (val)** (77.33), **LiveCodeBench v5** (57.77), **ChartQA** (90.88), and **Common Voice v16** (90.8) [10], [12]–[16], [25], [26].

Against GPT-4.1 on shared tasks we observe improvements of +3.0 (MMLU-Pro), +1.18 (MMLU), +2.53 (MMMU), +55.3 (AIME-2025), +15.01 (GPQA-Diamond), +12.07 (LiveCodeBench), and +5.61 (AI2D): a macro-average of **+13.53** points (median **+5.61**). Gains concentrate where structured tool context (OCR/diagram/chart parsing, retrieval, sandbox feedback) is most informative; coding shows headroom if longer agentic loops are permitted. This supports our central claim that most of the improvement comes from the small-model and tool stack and the way it compiles context, rather than from relying on a single larger general-purpose model.

In our experiments with ablations, we observed: removing OCR/diagram/chart parsers drops AI2D/ChartQA by 4–7 points; disabling context compilation costs  $\approx 2$  points on GPQA-Diamond; turning off the optional short reasoning head hurts AIME and MMLU-Pro in high-difficulty slices. Together, specialized model selection chain + tool context + bounded reasoning explain the observed improvements while keeping most traffic on cheaper SLM paths.

### A. Per-domain notes

On knowledge and general reasoning, we top the group on **MMLU** by +1.18 over GPT-4.1 and +2.18 over Gemini 2.5 Pro. The harder **MMLU-Pro** clusters us with Sonnet 4 and its Thinking variant, within 2.6 points of the best. In practice, most items resolve on SLM+tool routes, with the controller only invoking more aggressive tool chains when predicted difficulty and uncertainty spike [10], [25].

TABLE II  
HEAD-TO-HEAD BENCHMARK RESULTS (HIGHER IS BETTER, %).

Benchmark	Interfaze-Beta	GPT-4.1	GPT-5 (Minimal Reasoning)	Claude Sonnet 4	Gemini 2.5 Flash	Claude Sonnet 4 (Thinking)	Claude Opus 4 (Thinking)	Gemini 2.5 Pro
MMLU-Pro	83.6	80.6	80.6	83.7	80.9	83.7	86.0	86.2
MMLU	<b>91.38</b>	90.2	—	—	—	88.8	89.0	89.2
MMMU (val)	77.33	74.8	—	—	79.7	74.4	76.5	82.0
AIME-2025	<b>90.0</b>	34.7	31.7	38.0	60.3	74.3	73.3	87.7
GPQA-Diamond	81.31	66.3	67.3	68.3	68.3	77.7	79.6	84.4
LiveCodeBench v5	57.77	45.7	55.8	44.9	49.5	65.5	63.6	75.9
ChartQA	<b>90.88</b>	—	—	—	—	—	—	—
AI2D	<b>91.51</b>	85.9	—	—	—	—	—	89.5
Common Voice v16	<b>90.8</b>	—	—	—	—	—	—	—

For graduate-level science (**GPQA-Diamond**), our 81.31 represents a +15.01 lift over GPT-4.1 and lands within 3.09 of Gemini 2.5 Pro. The gains concentrate on difficult items where retrieval plus compact context compilation provide verifiable evidence [12].

On competition math (**AIME-2025**), we obtain 90.0 a wide margin of +55.3 versus GPT-4.1 and +16–17 versus Sonnet 4 and Opus 4 (Thinking). The router prefers math-focused tools and enables short self-consistency only when arithmetic checks disagree, which curbs near-miss numeric errors.

For coding (**LiveCodeBench v5**), 57.77 comfortably beats GPT-4.1 (+12.07), Sonnet 4 (+12.87), and Gemini 2.5 Flash (+8.27) but trails the most aggressive code-specialized systems Sonnet 4 (Thinking) by 7.73 and Gemini 2.5 Pro by 18.13. This reflects a deliberate choice to favor lightweight sandbox checks over longer agentic debugging loops [13].

In multimodal perception, **MMMU (val)** reaches 77.33 (+2.53 over GPT-4.1), with the largest margins on **AI2D** (91.51: +5.61 over GPT-4.1 and +2.01 over Gemini 2.5 Pro) and strong **ChartQA** (90.88). Structured OCR text, bounding boxes, chart axes, and object relations merged into compact prompts that reduce hallucination and support numerical comparisons [14]–[16].

For speech, **Common Voice v16** reaches 90.8 using a multilingual ASR specialist trained on large multilingual audio datasets [26].

## VI. LIMITATIONS AND FUTURE WORK

We see two practical pain points: *delay* and *over-building of context*. Delay stems from context fan out from SLMs (OCR/ASR, scraping, retrieval) and the bounded agentic loop, plus cold starts for small models hosted on our inference infrastructure, which can push tail latency even when average costs are low. Over-building happens when the controller invokes more tools or retrieval passes than are needed for a given query, inflating cost without clear quality gains [2], [3]. In future work, we will treat delay and over-building as key objectives: we will make aggressive context construction opt-in, add small penalties for extra tool invocations in the controller’s cost model, and track “avoidable context expansions” (cases where a cheaper tool chain would have passed the accuracy bar) [2], [3].

## ACKNOWLEDGMENTS

We thank the colleagues and reviewers who provided detailed feedback on early drafts and helped improve the

clarity, presentation, and technical framing of our work. We also thank everyone who assisted with internal review, benchmarking discussions, and paper editing.

## REFERENCES

- [1] A. Clark, D. de las Casas, A. Guy, A. Mensch, M. Paganini, J. Hoffmann, B. Damoc, B. Hechtman, T. Cai, S. Borgeaud, *et al.* Unified Scaling Laws for Routed Language Models. In *Proceedings of the 39th International Conference on Machine Learning (ICML)*, 2022. URL: <https://proceedings.mlr.press/v162/clark22a.html>.
- [2] L. Chen, M. Zaharia, and J. Zou. FrugalGPT: How to Use Large Language Models While Reducing Cost and Improving Performance. *arXiv:2305.05176*, 2023. URL: <https://arxiv.org/abs/2305.05176>.
- [3] D. Ding, A. Mallick, C. Wang, R. Sim, S. Mukherjee, V. Ruhle, L. V. S. Lakshmanan, and A. H. Awadallah. Hybrid LLM: Cost-Efficient and Quality-Aware Query Routing. In *International Conference on Learning Representations (ICLR)*, 2024. URL: <https://openreview.net/forum?id=02f3mUtqnm>.
- [4] W. Jitkrittum, *et al.* Universal Model Routing for Efficient LLM Inference. *arXiv:2502.08773*, 2025. URL: <https://arxiv.org/abs/2502.08773>.
- [5] T. Schick, J. Dwivedi-Yu, R. Dessi, R. Raileanu, M. Lomeli, L. Zettlemoyer, N. Cancedda, and T. Scialom. Toolformer: Language Models Can Teach Themselves to Use Tools. *arXiv:2302.04761*, 2023. URL: <https://arxiv.org/abs/2302.04761>.
- [6] Y. Shen, K. Song, X. Tan, D. Li, W. Lu, and Y. Zhuang. HuggingGPT: Solving AI Tasks with ChatGPT and its Friends in Hugging Face. *arXiv:2303.17580*, 2023. URL: <https://arxiv.org/abs/2303.17580>.
- [7] S. Yao, J. Zhao, D. Yu, N. Du, I. Shafran, K. Narasimhan, and Y. Cao. ReAct: Synergizing Reasoning and Acting in Language Models. *arXiv:2210.03629*, 2022. URL: <https://arxiv.org/abs/2210.03629>.
- [8] P. Lu, B. Peng, H. Cheng, M. Galley, K.-W. Chang, Y. N. Wu, S.-C. Zhu, and J. Gao. Chameleon: Plug-and-Play Compositional Reasoning with Large Language Models. *arXiv:2304.09842*, 2023. URL: <https://arxiv.org/abs/2304.09842>.
- [9] X. Wang, J. Wei, D. Schuurmans, *et al.* Self-Consistency Improves Chain of Thought Reasoning in Language Models. In *International Conference on Learning Representations (ICLR)*, 2023. URL: <https://arxiv.org/abs/2203.11171>.
- [10] Y. Wang, X. Ma, G. Zhang, Y. Ni, A. Chandra, S. Guo, W. Ren, A. Arulraj, X. He, Z. Jiang, *et al.* MMLU-Pro: A More Robust and Challenging Multi-Task Language Understanding Benchmark. *arXiv:2406.01574*, 2024. URL: <https://arxiv.org/abs/2406.01574>.
- [11] Art of Problem Solving (AoPS). AIME Problems and Solutions (1983 present). URL: [https://artofproblemsolving.com/wiki/index.php/AIME\\_Problems\\_and\\_Solutions](https://artofproblemsolving.com/wiki/index.php/AIME_Problems_and_Solutions).
- [12] D. Rein, B. L. Hou, A. C. Stickland, J. Petty, R. Y. Pang, J. Dirani, J. Michael, and S. R. Bowman. GPQA: A Graduate-Level Google-Proof Q&A Benchmark. *arXiv:2311.12022*, 2023. URL: <https://arxiv.org/abs/2311.12022>.
- [13] N. Jain, K. Han, A. Gu, W.-D. Li, F. Yan, T. Zhang, S. Wang, A. Solar-Lezama, K. Sen, and I. Stoica. LiveCodeBench: Holistic and Contamination Free Evaluation of Large Language Models for Code. *arXiv:2403.07974*, 2024. URL: <https://arxiv.org/abs/2403.07974>.

[14] X. Yue, Y. Ni, K. Zhang, T. Zheng, R. Liu, G. Zhang, S. Stevens, D. Jiang, W. Ren, Y. Sun, C. Wei, B. Yu, R. Yuan, R. Sun, M. Yin, B. Zheng, Z. Yang, Y. Liu, W. Huang, H. Sun, Y. Su, and W. Chen. MMMU: A Massive Multi-discipline Multimodal Understanding and Reasoning Benchmark for Expert AGI. In *Proceedings of the IEEE/CVF Conference on Computer Vision and Pattern Recognition (CVPR)*, 2024. URL: [https://openaccess.thecvf.com/content/CVPR2024/papers/Yue\\_MMMU\\_A\\_Massive\\_Multi-discipline\\_Multimodal\\_Understanding\\_and\\_Reasoning\\_Benchmark\\_for\\_CVPR\\_2024\\_paper.pdf](https://openaccess.thecvf.com/content/CVPR2024/papers/Yue_MMMU_A_Massive_Multi-discipline_Multimodal_Understanding_and_Reasoning_Benchmark_for_CVPR_2024_paper.pdf).

[15] A. Kembhavi, M. Salvato, E. Kolve, M. Seo, H. Hajishirzi, and A. Farhadi. A Diagram Is Worth A Dozen Images. *arXiv:1603.07396*, 2016. URL: <https://arxiv.org/abs/1603.07396>.

[16] A. Masry, D. X. Long, J. Q. Tan, S. Joty, and E. Hoque. ChartQA: A Benchmark for Question Answering about Charts with Visual and Logical Reasoning. *arXiv:2203.10244*, 2022. URL: <https://arxiv.org/abs/2203.10244>.

[17] V. Sanh, L. Debut, J. Chaumond, and T. Wolf. DistilBERT, a distilled version of BERT: smaller, faster, cheaper and lighter. *arXiv:1910.01108*, 2019. URL: <https://arxiv.org/abs/1910.01108>.

[18] Z. Sun, H. Yu, X. Song, R. Liu, Y. Yang, and D. Zhou. MobileBERT: a Compact Task-Agnostic BERT for Resource-Limited Devices. In *Proceedings of the 58th Annual Meeting of the Association for Computational Linguistics (ACL)*, 2020. URL: <https://arxiv.org/abs/2004.02984>.

[19] T. Schick and H. Schütze. It's Not Just Size That Matters: Small Language Models Are Also Few-Shot Learners. In *Proceedings of the 16th Conference of the European Chapter of the ACL (EACL)*, 2021. URL: <https://arxiv.org/abs/2009.07118>.

[20] C. Xu, Y. Xu, S. Wang, Y. Liu, C. Zhu, and J. McAuley. Small Models are Valuable Plug-ins for Large Language Models. In *Findings of the Association for Computational Linguistics*, 2024. URL: <https://aclanthology.org/2024.findings-acl.18/>.

[21] M. Li, J. Xiang, Q. Zhang, K. Wan, and X. Chen. Flipping Knowledge Distillation: Leveraging Small Models' Expertise to Enhance LLMs in Text Matching. In *Proceedings of the 63rd Annual Meeting of the ACL (Long Papers)*, 2025. URL: <https://aclanthology.org/2025.acl-long.1081/>.

[22] Z. Shen. LLM With Tools: A Survey. *arXiv:2409.18807*, 2024. URL: <https://arxiv.org/abs/2409.18807>.

[23] P. Belcak, G. Heinrich, S. Diao, Y. Fu, X. Dong, S. Muralidharan, Y. C. Lin, and P. Molchanov. Small Language Models are the Future of Agentic AI. *arXiv:2506.02153*, 2025. URL: <https://arxiv.org/abs/2506.02153>.

[24] Meta AI. Llama Guard 4: Multimodal safety classifier 12B, 2025. URL: <https://www.llama.com/docs/model-cards-and-prompt-formats/llama-guard-4/>.

[25] D. Hendrycks, C. Burns, S. Basart, A. Zheng, M. Stepanek, E. Kuba, S. Ball, S. Tran, C. Tang, J. Song, J. Kornblith, A. Chen, and J. Steinhardt. Measuring Massive Multitask Language Understanding. In *Proceedings of the International Conference on Learning Representations (ICLR)*, 2021. URL: <https://arxiv.org/abs/2009.03300>.

[26] R. Ardila, M. Branson, K. Davis, M. Henretty, M. Kohler, J. Meyer, R. Morais, L. Saunders, F. Tyers, and G. Weber. Common Voice: A Massively-Multilingual Speech Corpus. In *Proceedings of The 12th Language Resources and Evaluation Conference (LREC)*, 2020. URL: <https://arxiv.org/abs/1912.06670>.

[27] A. Radford, J. W. Kim, T. Xu, G. Brockman, C. McLeavey, and I. Sutskever. Robust Speech Recognition via Large-Scale Weak Supervision. *arXiv:2212.04356*, 2022. URL: <https://arxiv.org/abs/2212.04356>.

[28] B. Desplanques, J. Thienpondt, and K. Demuynck. ECAPA-TDNN: Emphasized Channel Attention, Propagation and Aggregation in TDNN-Based Speaker Verification. In *Proceedings of Interspeech*, 2020. URL: [https://www.isca-archive.org/interspeech\\_2020/desplanques20\\_interspeech.html](https://www.isca-archive.org/interspeech_2020/desplanques20_interspeech.html).

[29] H. Bredin. pyannote.audio 2.1 Speaker Diarization Pipeline: Principle, Benchmark, and Recipe. In *Proceedings of Interspeech*, 2023. URL: [https://www.isca-archive.org/interspeech\\_2023/bredin23\\_interspeech.html](https://www.isca-archive.org/interspeech_2023/bredin23_interspeech.html).

[30] M. Sharma *et al.* A Comprehensive Empirical Review of Modern Voice Activity Detection Approaches for Movies and TV Shows. Technical report, 2022.

[31] Silero AI. Silero VAD: Pre-trained Enterprise-Grade Voice Activity Detector. GitHub repository, accessed 2025. URL: <https://github.com/snakers4/silero-vad>.

[32] C. Li, W. Liu, R. Guo, X. Yin, K. Jiang, Y. Du, Y. Du, L. Zhu, B. Lai, X. Hu, D. Yu, and Y. Ma. PP-OCRv3: More Attempts for the Improvement of Ultra Lightweight OCR System. *arXiv:2206.03001*, 2022. URL: <https://arxiv.org/abs/2206.03001>.

[33] Y. Huang, L. Bi, F. Fang, S. Liu, X. Fang, X. Sun, and J. Liu. LayoutLMv3: Pre-training for Document AI with Unified Text and Image Masking. *arXiv:2204.08387*, 2022. URL: <https://arxiv.org/abs/2204.08387>.

[34] S. Marinai, E. Marinai, and colleagues. Machine Learning for Reading Order Detection in Document Image Understanding. In *Machine Learning in Document Analysis and Recognition*, 2008.

[35] L. Qiao, C. Li, Z. Cheng, Y. Xu, Y. Niu, and X. Li, "Reading order detection in visually-rich documents with multi-modal layout-aware relation prediction," *Pattern Recognition*, vol. 150, art. 110314, 2024. doi: 10.1016/j.patcog.2024.110314.

[36] Z. Wang, *et al.* LayoutReader: Pre-training of Text and Layout for Reading Order Detection. In *Proceedings of the 2021 Conference on Empirical Methods in Natural Language Processing (EMNLP)*, 2021. URL: <https://aclanthology.org/2021.emnlp-main.389/>.

[37] G. Kim, T. Kim, S. Park, S. Yun, C. D. Yoo, and N. I. Cho. OCR-free Document Understanding Transformer. In *European Conference on Computer Vision (ECCV)*, 2022. URL: [https://www.ecva.net/papers/eccv\\_2022/papers\\_ECCV/papers/136880493.pdf](https://www.ecva.net/papers/eccv_2022/papers_ECCV/papers/136880493.pdf).

[38] X. Zhai, B. Mustafa, A. Kolesnikov, and L. Beyer. Sigmoid Loss for Language Image Pre-Training. *arXiv preprint arXiv:2303.15343*, 2023. URL: <https://arxiv.org/abs/2303.15343>.

[39] N. Ravi, V. Gabeur, Y.-T. Hu, *et al.* SAM 2: Segment Anything in Images and Videos. *arXiv preprint arXiv:2408.00714*, 2024. URL: <https://arxiv.org/abs/2408.00714>.

[40] Baek, Lee, Han, Yun, and Lee. Character region awareness for text detection. In *Proceedings of the IEEE/CVF Conference on Computer Vision and Pattern Recognition (CVPR)*, pp. 9365–9374, 2019.

[41] JaidedAI. EasyOCR: Ready-to-use OCR with 80+ supported languages. GitHub repository, 2020. <https://github.com/JaidedAI/EasyOCR>.

[42] G. Jocher, A. Chaurasia, and J. Qiu. Ultralytics YOLOv8: Real-time object detection, Technical report, Ultralytics, 2023. <https://docs.ultralytics.com>.

[43] Y. Lu, J. Yang, Y. Shen, and A. H. Awadallah. OmniParser for Pure Vision-Based GUI Agent. *arXiv preprint arXiv:2408.00203*, 2024. URL: <https://arxiv.org/abs/2408.00203>.

[44] B. Xiao, H. Wu, W. Xu, X. Dai, H. Hu, Y. Lu, M. Zeng, C. Liu, and L. Yuan. Florence-2: Advancing a Unified Representation for a Variety of Vision Tasks. In *Proceedings of the IEEE/CVF Conference on Computer Vision and Pattern Recognition (CVPR)*, 2024. URL: [https://openaccess.thecvf.com/content/CVPR2024/papers/Xiao\\_Florence-2\\_Advancing\\_a\\_Unified\\_Representation\\_for\\_a\\_Variety\\_of\\_Vision\\_CVPR\\_2024\\_paper.pdf](https://openaccess.thecvf.com/content/CVPR2024/papers/Xiao_Florence-2_Advancing_a_Unified_Representation_for_a_Variety_of_Vision_CVPR_2024_paper.pdf).

[45] Q. Leng, J. Portes, S. Havens, M. Zaharia, and M. Carbin. Long Context RAG Performance of LLMs. Databricks Blog, 12 August 2024. Available at: <https://www.databricks.com/blog/long-context-rag-performance-l1ms>.

[46] J. Hron. Legal AI Benchmarking: Evaluating Long Context Performance for LLMs. Thomson Reuters Innovation Blog, 14 April 2025.

[47] P. Xu, W. Ping, X. Wu, L. McAfee, C. Zhu, Z. Liu, S. Subramanian, E. Bakhturina, M. Shoeybi, and B. Catanzaro. Retrieval Meets Long Context Large Language Models. *arXiv preprint arXiv:2310.03025*, 2023. Available at: <https://arxiv.org/abs/2310.03025>.